Science Bulletin 64 (2019) 1103–1109

Contents lists available at ScienceDirect

Science Bulletin

journal homepage: www.elsevier.com/locate/scib

Science Bulletin
www.scibull.com

Article

2-Methylimidazole assisted ultrafast synthesis of carboxylate-based metal–organic framework nano-structures in aqueous medium at room temperature

Shaheed Ullah, Bilal Akram, Hassan Ali, Hao Zhang, Haozhou Yang, Qingda Liu, Xun Wang *

Key Laboratory of Organic Opteoelectronics and Molecular Engineering, Department of Chemistry, Tsinghua University, Beijing 100084, China

ARTICLE INFO

Article history:
Received 29 January 2019
Received in revised form 21 March 2019
Accepted 29 May 2019
Available online 8 June 2019

Keywords:
Metal–organic framework
Carboxylate
2-Methylimidazole
Room temperature synthesis
Nanostructures

ABSTRACT

Carboxylate-based metal–organic frameworks (CMOFs) have received considerable attentions for their high stability, catalytic activity, and porosity. However, synthesis of CMOFs requires high temperature, pressure, and long reaction time. Here, we explored the activity of 2-methylimidazole (2-MIM) for ultrafast synthesis of CMOF nanostructures (CMOFNs), in aqueous medium at room temperature and reaction time of 10 min. Seven CMOFNs have been synthesized by using Al^{3+}, Cr^{3+}, Cu^{2+}, Fe^{3+}, In^{3+}, or Cd^{2+} salt and 1,4-bezenedicarboxylic acid, or 1,3,5-benzenetricarboxylic acid. Through this technique, the CMOFs with space time yield 181–501 kg m^{-3} day^{-1} and crystal sizes of ca. 200–700 nm was obtained.

1. Introduction

Carboxylate based metal–organic frameworks (CMOFs) have been widely studied because carboxylate ligands can be easily designed and synthesized in low cost and they can strongly coordinate with most metal ions to offer relatively high stability [1]. Because of these superior properties, CMOFs were applied in drug delivery, ion exchange, catalysis, energy storage, gas separation, chemical sensing, and water [2] and light harvesting [3]. The conventional synthesis methods limited the efficient production of CMOFs. Solvothermal synthesis requires high temperature, pressure, and a longer reaction time. For instance, [Al(OH)(BDC)] (MIL-53(Al), H_2BDC = 1,4-bezenedicarboxylic acid), $[Cr_3O(OH)(BDC)_3]$ (MIL-101) and $[Zr_6O_4(OH)_4(BDC)_6]$ (UiO-66) were obtained at high temperature and time of, 220 °C for 72 h, 220 °C for 8 h and 120 °C for 12 h, respectively [4]. The solid grinding [5], microemulsion method, ultrasound technique, and microwave synthesis are less time consuming, but the need for expensive instrumentation made them less desirable approaches [6]. Previously, the room temperature syntheses of CMOFs have been rarely performed [5–9]. Yet, development of a universal method for the efficient synthesis of CMOFs at room temperature remains a challenge. Besides, synthesis of nano scale CMOFs is highly desirable due to a better performance, compared to their bulk counterpart [8]. Our manipulation and understanding will enable the desirable room temperature synthesis of carboxylate metal-organic framework nanostructures (CMOFNs) in aqueous medium at room temperature with high efficiency.

Imidazole and its derivatives are mild Lewis bases, exhibit the conjugated acid pK_b of ~7. The basic site is the nitrogen with the lone pair, which yields imidazolium cation upon protonation. For example, in Henry reaction where imidazole deprotonates nitromethane and facilitates the formation of nitroaldol [10–14]. The lone pair of electrons on nitrogen of imidazole deprotonates available acid. Thus, we hypothesized that using imidazole could generate highly carboxylate active anion, by deprotonating the carboxylic acid, which can readily attack on available metal ion in solution and leads to room temperature synthesis of CMOFNs.

In recent years, our group has made great efforts to apply mixed metal approach [15] or competitive ligands coordination strategies for the design of MOF nanostructures [15–20]. On the other hand, the competing coordination between metal ions and modulators is also helpful to the synthesis of various MOFs [21,22]. In this study, we have developed a method for the room temperature synthesis of CMOFNs using 2-methylimidazole (2-MIM) as an additive in aqueous medium. Ten CMOFNs MIL-53(Al), [Cr(OH)(BDC)] (MIL-53(Cr)), [Fe(OH)(BDC)] (MIL-53(Fe)), $[Cu(H_2O)(BDC)]$ (Cu-BDC), UiO-66, [In(OH)(BDC)] (MIL-53(In)), $[Cd(H_2O)(BDC)]$ (Cd-BDC), $[Zn_4O(BTB)_2]$ (MOF-177), [Al(OH)(NDC)] (DUT-4), and $[Cu_3(BTC)_2]$

* Corresponding author.
E-mail address: wangxun@mail.tsinghua.edu.cn (X. Wang).

https://doi.org/10.1016/j.scib.2019.06.009
2095-9273/

(HKUST-1) were synthesized and characterized from 8 metal salts (Al^{3+}, Cr^{3+}, Cu^{2+}, Fe^{3+}, Zr^{4+}, In^{3+}, Zn^{2+}, Cd^{2+}) with 4 carboxylic acids (1,3,5-tris(4-carboxyphenyl)benzene = H_3BTB, 2,6-naphthalenedicarboxylic acid = H_2NDC, and 1,3,5-benzenetricarboxylic acid = H_3BTC). However, the method has limitations for the synthesis of CMOFNs, UiO-66, DUT-4, and MOF-177. Compared to conventional methods, the 2-MIM assisted synthesis is much faster and the reaction can be performed at room temperature (Fig. 1). The 2-MIM acts as a mild-base to deprotonate the acid. Moreover, the nitrogen in imidazole might also be possible to coordinate with the metal ions in a proper strength, serving as a modulator to control the growth of CMOFNs. The synthesized CMOFNs through this method have comparable properties to CMOFNs prepared by conventional methods.

2. Materials and methods

2.1. Materials

$FeCl_3·6H_2O$, $ZrCl_4$, $AlCl_3·6H_2O$, $Zn(NO_3)_2·6H_2O$, $Cu(NO_3)_2·3H_2O$, $Cr(NO_3)_3·9H_2O$, $In(NO_3)_3·3H_2O$, $CdCl_2·5H_2O$, 2-MIM, H_2BDC, H_2NDC, H_3BTC, H_3BTB, *N*,*N*-dimethylformamide (DMF), NaOH and ethanol were purchased from Alfa Aesar and Sinopharm. All chemicals were purchased in analytical grade and used without any further purification.

2.2. Synthesis of CMOFNs

All CMOFNs were prepared in the same method, and the procedure for MIL-53(Al) is described in detail here. In a typical synthesis, 2-MIM (0.01, 0.12 mmol) and H_2BDC (0.016 g, 0.1 mmol) solution was prepared in water (4 mL) and sonicated for 10 min (notes: H_2BDC cannot fully dissolve without the adding of 2-MIM). Similarly, the $AlCl_3$ solution was obtained by dissolving the $AlCl_3·6H_2O$ (0.024 g, 0.1 mmol) in water (2 mL). Subsequently, all the metal salt solution was added drop wise to the 2-MIM/H_2BDC solution under continuous sonication. The mixture was left over at sonication for 10 min and then the precipitate was separated by centrifugation and washed with DMF (one time) and ethanol (twice). The precipitate of CMOFNs was dried at 80 °C for 12 h and activated in vacuumed oven at 150 °C for 4 h. Yield was 60% (12.56 mg) based on $AlCl_3·6H_2O$. For other CMOFNs, the metal salt and carboxylic acid ligand were replaced accordingly. Yield for MIL-53(Cr), MIL-53(Fe), Cu-BDC, and UiO-66 were 51% (11.8 mg), 63% (14.9 mg), 86% (20.9 mg), and 30% (8 mg), respectively, based on their metal salts.

The space time yield (STY in kg m^{-3} day^{-1}) of CMOFNs was calculated using the following equation and their values are tabulated in Table S1 (online).

$$STY = \left(\frac{M}{V\tau}\right) \times 1.44 \times 10^6,$$

where *M*, *V*, and τ are mass (g) of dried MOF, volume (cm^{-3}) of the solution, and reaction time (min) [23].

The details of other controlled experiments are listed in Tables S2–S5 (online) in the Supporting Information.

2.3. Instrumentation

The post-reaction filtrate was obtained and a 50 μL of the filtrate was diluted with 1 mL ethanol. The quantitative consumption of the organic reactants/reagents, such as H_2BDC and 2-MIM during the reaction was calculated from the peak area obtained from the post- and pre-reaction filtrate obtained with a ISQ GC–MS with an ECD detector (Thermo Trace GC Ultra) having capillary column (Thermo Scientific, TR-5MS, length 30 m, i.d. 0.25 mm, film 0.25 μm). Transmission electron microscopy (TEM) was conducted through a HITACHI H-7700 TEM equipped with energy-dispersive spectroscopy (EDS) an accelerating voltage of 100 kV. X-ray photoelectron spectroscopy (XPS) was performed using scanning X-ray microprobe (Quantera SXM, ULVAC-PHI, INC) operated at 250 kV, 55 eV with monochromatic Al Kα radiation. The C 1 s peak at 284.8 eV was used as a reference for binding energies correction. Powder X-ray diffraction of samples were recorded using Bruker D8-advance X-ray powder diffractometer with Cu Kα radiation (λ = 1.5406 Å) at 40 kV and 150 mA current. TA-50 thermal analyzer was used for thermogravimetric analysis at constant heating rate 10 °C min^{-1} from room temperature to 800 °C. The FT-IR spectra were obtained in transmission mode on a Perkin-Elmer Spectrum 100 spectrometer (Waltham, MA, USA). The data was obtained in the range of 400–4,000 cm^{-1} for FT-IR analysis with resolution of 4 cm^{-1}. To evaluate Brunauer-Emmett-Teller (BET) surface area Quadasorb SI-MP was used and pore volume was calculated using Saito-Foley (SF) and BJH methods. N_2 was used as the adsorbate gas. The scanning electron microscopy (SEM) was performed using Hitachi SU8010. The elemental mapping was performed using X-ray spectrometer (JEOL 200F) operating at 200 kV. For pH measurement a Mettler Toledo Delta 320 pH Meter was used.

3. Results and discussion

Optimal reaction condition was achieved for MIL-53(Al) and similar conditions were applied to other MOFs. Different conditions were used, firstly amount of $AlCl_3·6H_2O$ was kept constant while amount of 2-MIM and H_2BDC were changed to get to optimal condition (Table S2 online). As show in powder x-ray diffraction (PXRD) pattern (Fig. 2), irregular and not well crystallized structures were obtained at conditions (1–5) and (7–9), while uniform regular morphology was obtained at condition (6): 0.01 g 2-MIM + 0.016 g H_2BDC (4 mL H_2O) + 0.024 g $AlCl_3·6H_2O$ (2 mL H_2O). Further, effect of increase or decrease in concentration of $AlCl_3·6H_2O$ for MIL-53(Al) synthesis was studied. The PXRD spectra (1–4)

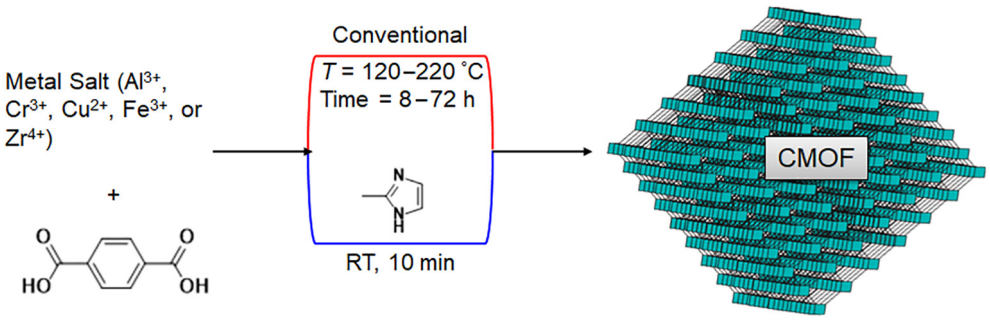

Fig. 1. (Color online) Schematic of CMOFs synthesis via conventional and 2-MIM assisted method.

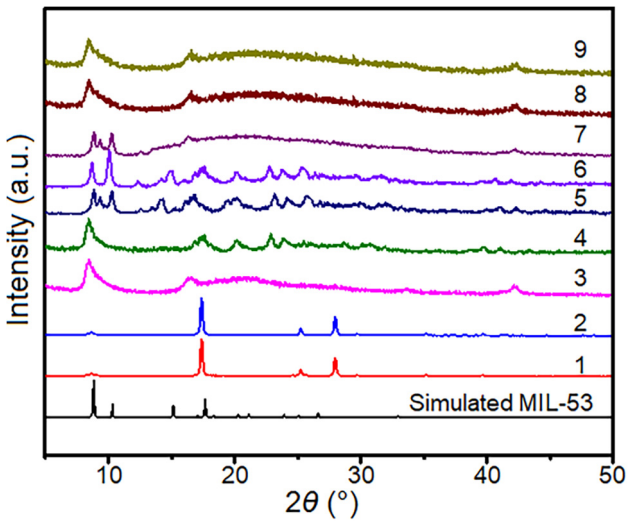

Fig. 2. (Color online) PXRD pattern of MIL-53(Al) at different 2-MIM and H_2-BDC ratios and concentrations (ratio of 2-MIM:H_2BDC from condition 1 to 9 is 5:95, 10:90, 20:80, 40:60, 60:40, 80:20, 90:10, respectively). The experiment details are listed in Table S2 (online).

(Fig. S1 online) shows structural changes by varying amount $AlCl_3 \cdot 6H_2O$ as detailed in Table S3 (online). Results indicated that either increase or decrease in metal salt concentration alters the product structure. Though the main PXRD peak corresponding to MOF formation was present in each case but the smaller peaks overlapped to form broad peak, which might be due to no proper development of crystal phases. No obvious change was observed by change the solvent amount. Furthermore, time controlled experiments were performed as detailed in (Table S4 online). The PXRD results showed that prolonging the reaction time have no influence upon the 2-MIM assisted synthesis of CMOFN synthesis of MIL-53(Al) (Fig. S2 online). However, short time (less than 10 min) led to no proper structure formation, which could be due to incomplete reaction. Therefore, the concentration and ratio of different precursors were optimized and this condition was utilized for CMOFNs synthesis in all following experiments or otherwise specified.

To confirm the composition of the prepared CMOFNs, GC–MS and other characterization techniques were utilized. GC–MS was used to check the utilization of 2-MIM and H_2BDC. Results showed that pre-reaction mixture without metal consisted of 60% 2-MIM and 40% H_2BDC (Fig. 3a). The relative post-reaction concentration of 2-MIM and H_2BDC were 94%±1% and 5%±1%, respectively. The 2-MIM concentration before and after reaction remained unchanged, allude the absence of 2-MIM in the final product. Furthermore, MIL-53(Al), MIL-53(Cr), MIL-53(Fe), Cu-BDC, and UiO-66 CMOFNs were analyzed through XPS, FT-IR and EDS. The XPS spectra showed the corresponding peaks of metal, carbon (C), and oxygen (O) (Fig. 3b). Previous reports suggested that nitrogen containing MIL 53(Cr) has an additional binding energy peak at 400 eV, however, here no peaks were observed at ~400 eV, corresponding to nitrogen [24], in any of the spectra, which confirmed the absence of 2-MIM in the final product. Only C, O and corresponding metal signals were existed in the spectra [25–28]. Similar results were obtained using EDS elemental mapping (Fig. S3 online). The absence of 2-MIM in the CMOFNs was further verified through UV–visible spectroscopy (Fig. 3c). The 2-MIM exhibit maximum absorbance peak at wavelength (λ) around 206 nm while mixture of 2-MIM and H_2BDC show peaks at λ = 206 and 240 nm respectively. The UV–visible spectra of post-reaction supernatant of CMOFNs showed the visible peak of 2-MIM of the same absor-

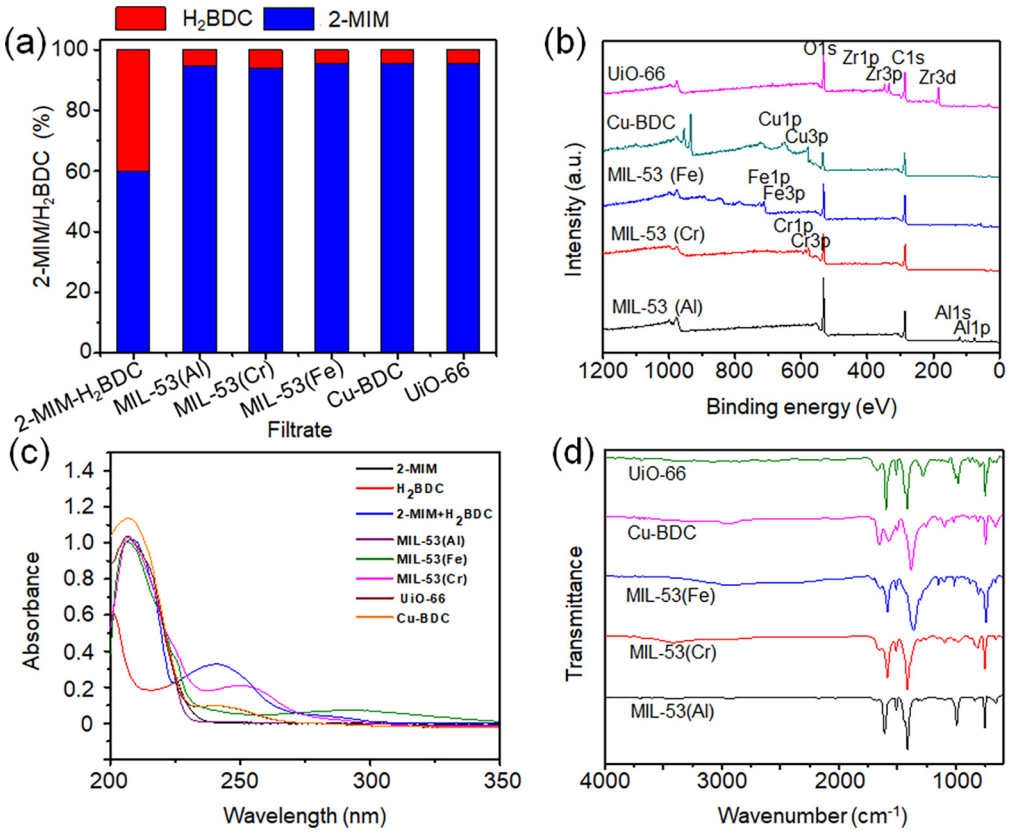

Fig. 3. (Color online) (a) GC–MS of the pre-reaction MIM-H_2BDC solution and post-reaction filtrates. (b) XPS, (c) UV–visible, and (d) FT-IR of CMOFNs of MIL-53(Al), MIL-53 (Cr), MIL-53(Fe), Cu-BDC, and UiO-66.

bance as of pre-reaction, while in each case the H_2BDC peak was not present showing the utilization of H_2BDC. FTIR spectroscopy of the CMOFNs was performed to locate the atomic bonding within the molecules (Fig. 3d). The FTIR spectrum for MIL-53(Al) shows the Al-O-C symmetric and asymmetric stretching peaks at 1,413 and 1,603 cm^{-1}. Similarly, Cr-O-C show the characteristic peaks at 1,500 to 1,600 cm^{-1}, the Fe-O-C peaks were found at 1,581, and 1,514 cm^{-1}, and Cu-O-C vibration peaks were observed at 1,576 and 1,640 cm^{-1}. The vibrational peaks for UiO-66 were observed at 1,500 cm^{-1} corresponding to the Zr-O-C stretching while a small peak at 1,670 cm^{-1} may be due to the traces of non-bonded H_2BDC. These results are in correlation with the reported literature [29–33]. Besides, no prominent vibrational peaks for N-bonded atoms were observed, which suggests that 2-MIM acted as an additive, very likely the deprotonating agent, for the CMOFN synthesis.

To study the role of 2-MIM, NaOH and $NH_3{\cdot}H_2O$ were used to replace the 2-MIM. Firstly different amounts of NaOH were used as detailed in Table S5 (online). No prominent peak was observed in the PXRD pattern, revealed the nearly amorphous nature of the product (Fig. S4 online). This may be due to the fast deprotonation of H_2BDC in the presence of NaOH, or the hydrolysis of metal ions. Thus, only mild base is suitable for the synthesis of CMOFNs. Furthermore, $NH_3{\cdot}H_2O$ was also used as a mild base to substitute 2-MIM, however, no products can be collected. The reason behind might be that NH_3 would coordinated strongly with metal ions, impeding the formation of corresponding metal-carboxylate coordination. These results might suggest that strong coordination is not suitable for the preparation of CMOFNs.

The 2-MIM is certain to act as a base and attracts a proton from the COOH group of a carboxylate ligand. The negatively charged ligand then forms a complex with the metal ions. The 2-MIM cation can form a 2-MIM salt with the anion of the metal salts. The acidic medium could inhibit and the basic medium may elevate the CMOFNs formation. For the proof of concept, the CMOFN syntheses were performed at pH = 2 and 12 by adding proper amount of HCl or NaOH solutions prior to addition of the metal salt (Figs. S5 and S6 online), whereas, other reaction parameters such as reaction time, molar ratio and concentration of reactants, were kept constant. No CMOFNs formation occurred at pH = 2. Contrary, high yield but amorphous product was obtained in a basic medium pH = 12, elude the possibility of CMOFNs formation in a strong basic medium. These results confirmed that the CMOFN synthesis at room temperature benefited from the mild basic nature of 2-MIM and provided an easy pathway for the efficient synthesis of CMOFNs.

The size and shape of a MOF determines its physicochemical properties and relevance for various applications. The size defines the confinement of electrons, surface-to-bulk atomic ratio, and proportion of different atoms located at a specific site, whereas, the shape shows the type and arrangement of atoms on the surface. Therefore, the MOFs with well-defined morphology are highly desirable. Fig. 4 shows the TEM and Fig. S7 (online) SEM images of various CMOFNs obtained in this study. The MIL-53(Al), MIL-53 (Cr), and MIL-53(Fe) exhibit one-dimensional porous channels. These structures were formed due to interconnection of Al^{3+}, Cr^{3+}, and Fe^{3+} octahedral corner sharing through OH^- group with terephthalate ion and the two carboxylate anions of each BDC^{2-} form linkage to the adjacent Al^{3+}, Cr^{3+}, or Fe^{3+} cations [29,32,34]. The two dimensional nano-sheets were obtained for Cu-BDC. In this structure the coordination of terephthalate ion to a copper dimer is through bidentate bridging. Cu-BDC contains Cu^{2+} ions with lamellar geometry responsible for the 2D square-pyramidal channels giving 2D sheet morphology. These sheets then form week staking interaction to each other, like that of MOF-2 [31]. In contrast, the UiO-66 exhibits powder like morphology. In UiO-66 Zr^{4+} is coordinated to BDC^{2-} through two carboxylate ions but lack of long range order with in the structure [30]. However, the morphology of UiO-66 obtained through our method was not comparable to reported structure, suggested the limitation of this technique for the synthesis of UiO-66.

Furthermore, the MIL-53(Al), MIL-53(Cr), MIL-53(Fe), Cu-BDC and UiO-66 CMOFNs were characterized by PXRD (Fig. 5). The PXRD pattern of MIL-53(Al), MIL-53(Cr), MIL-53(Fe) and Cu-BDC show well defined sharp peaks confirmed the crystalline nature of these MOFs. All the main peaks were comparable with simulated pattern of previous literature and the PXRD study confirmed formation of respective CMOFNs [26,27,29–32,35]. Whereas, UiO-66 has an amorphous structure and a broad Bragg peak could be observed in PXRD not well comparable to the simulated pattern which shows that UiO-66 has not formed properly [35].

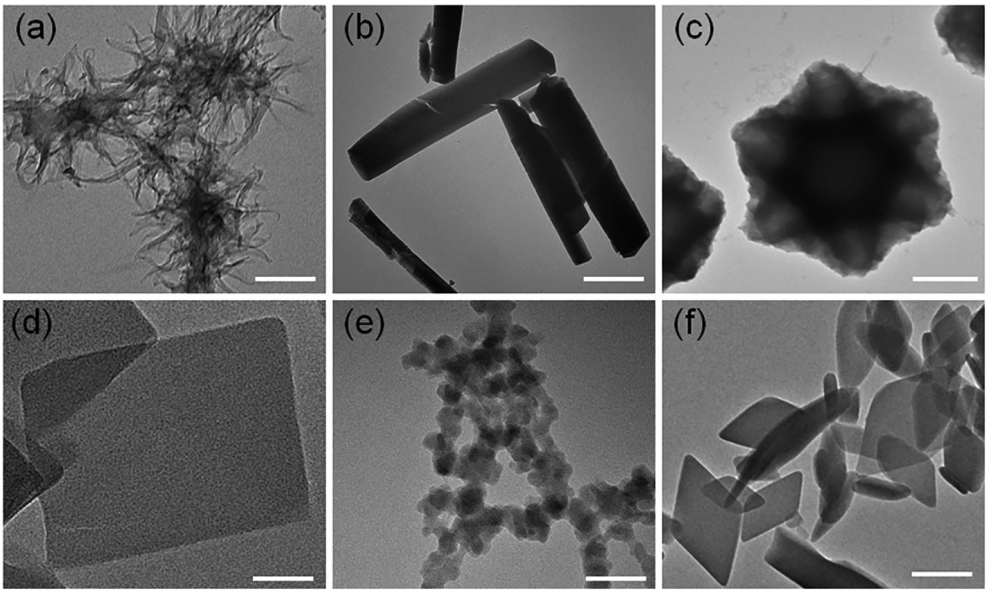

Fig. 4. TEM images of (a) MIL-53(Al), (b) MIL-53(Cr), (c) MIL-53(Fe), (d) Cu-BDC, (e) UiO-66, and (f) Cd-BDC MOFNs. The scale bars are 200 nm.

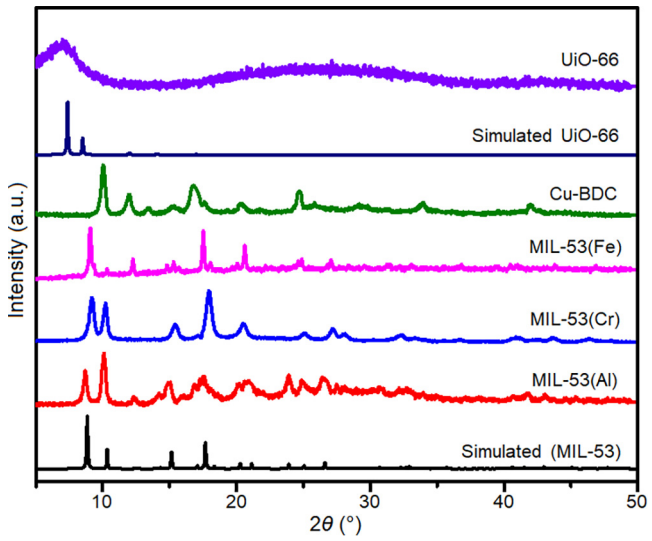

Fig. 5. (Color online) Powder XRD spectra and simulated spectra of CMOFNs.

Thermal stability of MOFs is important and a basic characteristic that MOF should possess, making it suitable for different applications in harsh environments. Thermal stability is evaluated on the basis of strong metal-ligand coordination, metal nodes, and the type of organic ligand. Carboxylate based ligands can be considered as hard Lewis bases forming strong bonds with Lewis acids, and this phenomenon makes CMOFs thermally stable. Thermogravametric analysis was performed to analyze the thermal stability of the synthesized CMOFNs. The thermograms show that all CMOFNs have good thermal stabilities (Fig. 6a). The MIL-53(Al) shows 18% reduction in weight, at a temperature around 200 °C due to the loss of trapped solvent in the crystal grooves and 60% weight loss, at a temperature around 550 °C, is due to the decomposition of the framework. Similarly, MIL-53(Cr), MIL-53(Fe) and Cu-BDC CMOFNs showed initial loss of solvent at ~200 °C and the framework decomposition at a temperature around 400, 420, and 350 °C respectively. However, minute weight loss for UiO-66 was observed even at a temperature > 600 °C. During thermogravimetric analysis weight loss of MOFs can be divided into three regions. The first loss below 100 °C considered being guest molecules removal, second loss below 200 °C is usually due to loss of coordinated solvent molecules, and the third region was assigned to framework degradation [36]. The conventionally synthesized MIL-53(Al, Fe or Cr) showed framework degradation from 400 to 550 °C, Cu-BDC above 300 °C, and UiO-66 above 500 °C [27,29,31,32]. The thermograms of CMOFNs in this work showed the framework degradation in the same regions, indicated that CMOFNs have comparable stability except UiO-66 [35] to conventionally synthesized CMOFs.

Moreover, most bivalent metal containing MOFs have poor hydrothermal and chemical stability due to hydrolysis of metal-linker bond, which could result in protonated ligand in an acidic medium or hydrated metallic nodes in a basic medium. Hence, they show stability only in mild neutral aqueous conditions [4,36,37]. To assess the water stability of 2-MIM assisted CMOFNs, we socked these MOFs in water for 72 h at room temperature. No obvious change in the PXRD patterns of these CMOFNs as function of time was observed, indicated the stability of these CMOFNs in an aqueous medium (Fig. S8 online).

One of the fundamental properties of MOF is its porosity. The CMOFNs also show permanent porosity attributes to well defined pore channels, making them suitable for gas storage, separation, and absorption of other small molecules. The Brunauer-Emmett-Teller (BET) analysis was performed to explore the surface area (Fig. 6b). The MIL-53(Al), MIL-53 (Cr), MIL-53(Fe), Cu-BDC and UiO-66 CMOFNs have surface area of 948, 1,193, 860, 613, and 181 $m^2 g^{-1}$, respectively. The adsorption desorption isotherm plot for MIL-53(Al), MIL-53(Cr), MIL-53(Fe) and Cu-BDC show hysteresis curves, which represent micro and meso porosity, also hysteresis loop suggests homogeneity in crystal size. The data obtained in our study was comparable to the reported literature [30,31,33,38]. On the other hand, UiO-66 shows comparatively low surface area, indicated that there is no long ordered porosity and the structure [35]. The pore distributions are listed in Fig. S9 (online). The pore volume was calculated using Barrett-Joyner-Halenda (BJH) and Saito-Foley (SF) method. The pore volume of MIL-53(Al), MIL-53 (Cr), MIL-53(Fe), Cu-BDC and UiO-66 CMOFNs obtained in this study was 0.41, 0.43, 0.40, 0.20 and 0.018 $cm^3 g^{-1}$, respectively.

In order to explore the applicability of this method, various other CMOFNs such as, MIL-53(In), Cd-BDC, DUT-4, HKUST-1 and MOF-177 were synthesized. The TEM images (Fig. S10 online) show the nano-belt, rods, and irregular spherical and cubic morphology for MIL-53(In), HKUST-1, DUT-4, and MOF-177, respectively. While TEM image (Fig. 4f) show 2D sheets formed in case of Cd-BDC. Furthermore, PXRD of these CMOFNs (Fig. S11 online), showed well resolved peaks of crystalline nature. The results were comparable to simulated pattern and reported literature [6,7,24,28,39–41] which confirmed the successful synthesis of these CMOFNs except DUT-4 and MOF-177.

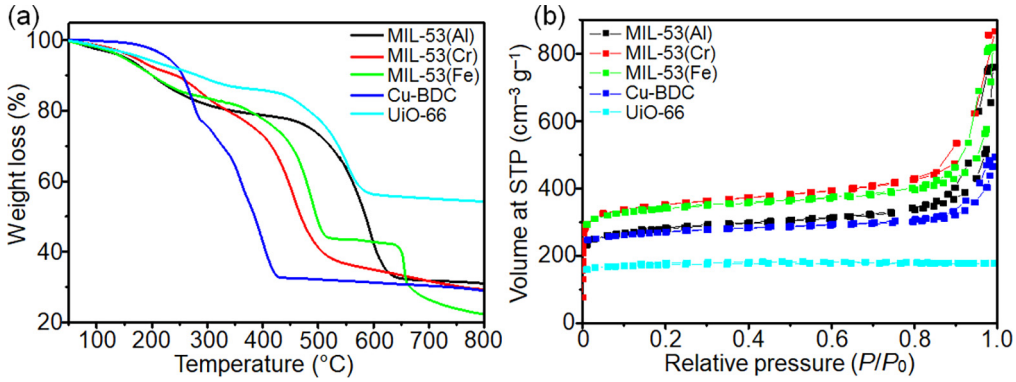

Fig. 6. (Color online) TGA plots (a) and BET surface area (b) of CMOFNs.

4. Conclusion

We successfully explored the capability of 2-MIM for the CMOFNs synthesis in aqueous medium at room temperature. Various CMOFNs from 6 metal salts (Al^{3+}, Cr^{3+}, Cu^{2+}, Fe^{3+}, In^{3+}, Cd^{2+}) with 2 carboxylic acids (H_2BDC, and H_3BTC) were successfully synthesized. However, limitation of the method was observed for the synthesis of CMOFNs, UiO-66, DUT-4, and MOF-177. The CMOFNs of well-defined morphology can be obtained in a short time of 10 min. The increase in 2-MIM concentration in the medium reduced the time of reaction. The synthesis of CMOFNs was inhibited in acidic environment, while enhanced in basic medium. However, the highly basic conditions disturbed the morphology of the product. These results suggested that, 2-MIM provides excellent platform for CMOFNs synthesis at room temperature, and may find a new order in industrial applications.

Conflict of interest

The authors declare that they have no conflict of interest.

Acknowledgments

This work was supported by the National Key R&D Program of China (2017YFA0700101 and 2016YFA0202801), and the National Natural Science Foundation of China (21431003).

Author contributions

Shaheed Ullah and Xun Wang coordinated and conceived the project. Shaheed Ullah designed and performed the experiments. Shaheed Ullah, Bilal Akram, and Hassan Ali, wrote and finalized the contents of the manuscript. Hao Zhang, Haozhou Yang, and Qingda Liu helped in data analysis and correction of the manuscript. All authors read and agreed to the final contents of the study.

Appendix A. Supplementary data

Supplementary data to this article can be found online at https://doi.org/10.1016/j.scib.2019.06.009.

References

[1] Yaghi OM, Okeeffe M, Ockwig NW, et al. Reticular synthesis and the design of new materials. Nature 2003;423:705–14.
[2] Kim H, Yang S, Rao SR, et al. Water harvesting from air with metal-organic frameworks powered by natural sunlight. Science 2017;356:430–4.
[3] Lee CY, Farha OK, Hong BJ, et al. Light-harvesting metal–organic frameworks (MOFs): efficient strut-to-strut energy transfer in bodipy and porphyrin-based mofs. J Am Chem Soc 2011;133:15858–61.
[4] Yuan S, Feng L, Wang K, et al. Stable metal–organic frameworks: design, synthesis, and applications. Adv Mater 2018;30:1704303.
[5] Leng K, Sun Y, Li X, et al. Rapid synthesis of metal–organic frameworks MIL-101(Cr) without the addition of solvent and hydrofluoric acid. Cryst Growth Des 2016;16:1168–71.
[6] Zhuang J-L, Ceglarek D, Pethuraj S, et al. Rapid room-temperature synthesis of metal–organic framework HKUST-1 crystals in bulk and as oriented and patterned thin films. Adv Funct Mater 2011;21:1442–7.
[7] Tranchemontagne DJ, Hunt JR, Yaghi OM. Room temperature synthesis of metal-organic frameworks: MOF-5, MOF-74, MOF-177, MOF-199, and IRMOF-0. Tetrahedron 2008;64:8553–7.
[8] Noh H, Kung C-W, Islamoglu T, et al. Room temperature synthesis of an 8-connected zr-based metal–organic framework for top-down nanoparticle encapsulation. Chem Mater 2018;30:2193–7.
[9] Sánchez-Sánchez M, Getachew N, Díaz K, et al. Synthesis of metal–organic frameworks in water at room temperature: salts as linker sources. Green Chem 2015;17:1500–9.
[10] Guan JT, Song XM, Zhang ZY, et al. Catalytic activity of 1-methylimidazole-based phosphine ligands in the palladium-catalyzed suzuki coupling reaction. Appl Organomet Chem 2015;29:87–9.
[11] Adib M, Mohammadi B, Sheikhi E, et al. 1-Methylimidazole-catalyzed reaction between tosylmethyl isocyanide and dialkyl acetylenedicarboxylates: an efficient synthesis of functionalized pyrroles. Chin Chem Lett 2011;22:314–7.
[12] Jones S, Northen J, Rolfe A. Catalytic phosphorylation using a bifunctional imidazole derived nucleophilic catalyst. Chem Commun 2005;30:3832–4.
[13] Nieri P, Carpi S, Fogli S, et al. Cholinesterase-like organocatalysis by imidazole and imidazole-bearing molecules. Sci Rep 2017;7:45760.
[14] Phukan M, Jyoti Borah K, Borah R. Imidazole-catalyzed henry reactions in aqueous medium. Synth Commun 2008;38:3068–73.
[15] Yang H, Wang B, Li H, et al. Trimetallic sulfide mesoporous nanospheres as superior electrocatalysts for rechargeable Zn-air batteries. Adv Energy Mater 2018;8:1801839.
[16] Wang X, He S, Chen Y, et al. Competitive coordination strategy for the synthesis of hierarchical-pore metal–organic framework nanostructures. Chem Sci 2016;7:7101–5.
[17] He T, Ni B, Xu X, et al. Competitive coordination strategy to finely tune pore environment of zirconium-based metal–organic frameworks. ACS Appl Mater Interfaces 2017;9:22732–8.
[18] He T, Xu X, Ni B, et al. Metal–organic framework based microcapsules. Angew Chem Int Ed 2018;57:10148–52.
[19] He T, Ni B, Zhang S, et al. Ultrathin 2D zirconium metal–organic framework nanosheets: Preparation and application in photocatalysis. Small 2018;14:1703929.
[20] He T, Chen S, Ni B, et al. Zirconium-porphyrin-based metal–organic framework hollow nanotubes for immobilization of noble-metal single atoms. Angew Chem Int Ed 2018;57:3493–8.
[21] Schaate A, Roy P, Godt A, et al. Modulated synthesis of Zr-based metal–organic frameworks: from nano to single crystals. Chem Eur J 2011;17:6643–51.
[22] Guo H, Zhu Y, Qiu S, et al. Coordination modulation induced synthesis of nanoscale $Eu_{1-x}Tb_x$-metal–organic frameworks for luminescent thin films. Adv Mater 2010;22:4190–2.
[23] Duan C, Li F, Xiao J, et al. Rapid room-temperature synthesis of hierarchical porous zeolitic imidazolate frameworks with high space-time yield. Sci China Mater 2017;60:1205–14.
[24] Feng Y, Wang T, Li Y, et al. Steering metallofullerene electron spin in porous metal–organic framework. J Am Chem Soc 2015;137:15055–60.
[25] Ge J, Liu L, Qiu L, et al. Facile synthesis of amine-functionalized MIL-53(Al) by ultrasound microwave method and application for CO_2 capture. J Porous Mater 2016;23:857–65.
[26] Vougo-Zanda M, Huang J, Anokhina E, et al. Tossing and turning: guests in the flexible frameworks of metal (III) dicarboxylates. Inorg Chem 2008;47:11535–42.
[27] Hou S, Wu Y, Feng Green L, et al. Synthesis and evaluation of an iron-based metal–organic framework MIL-88B for efficient decontamination of arsenate from water. Dalton Trans 2018;47:2222–31.
[28] McKellar SC, Graham AJ, Allan DR, et al. The effect of pressure on the post-synthetic modification of a nanoporous metal–organic framework. Nanoscale 2014;6:4163–73.
[29] Loiseau T, Serre C, Huguenard C, et al. A rationale for the large breathing of the porous aluminum terephthalate (MIL-53) upon hydration. Chem Eur J 2004;10:1373–82.
[30] Yang F, Li W, Tang B. Facile synthesis of amorphous UIO-66 (Zr-MOF) for supercapacitor application. J Alloys Compd 2018;733:8–14.
[31] Carson CG, Hardcastle K, Schwartz J, et al. Synthesis and structure characterization of copper terephthalate metal–organic frameworks. Eur J Inorg Chem 2009:2338–43.
[32] Serre C, Millange F, Thouvenot C, et al. Very large breathing effect in the first nanoporous chromium(III)-based solids: MIL-53 or $Cr^{III}(OH)(BDC)_x{\cdot}H_2O_y$. J Am Chem Soc 2002;124:13519–26.
[33] Cai X, Lin J, Pang M. Facile synthesis of highly uniform Fe-MIL-88B particles. Cryst Growth Des 2016;16:3565–8.
[34] Ma M, Noei H, Mienert B, et al. Iron metal–organic frameworks MIL-88B and NH_2-MIL-88B for the loading and delivery of the gasotransmitter carbon monoxide. Chem Eur J 2013;19:6785–90.
[35] Cavka JH, Jakobsen S, Olsbye U, et al. A new zirconium inorganic building brick forming metal organic frameworks with exceptional stability. J Am Chem Soc 2008;130:13850–1.
[36] Howarth AJ, Liu Y, Li P, et al. Chemical, thermal and mechanical stabilities of metal–organic frameworks. Nat Rev Mater 2016;1:15018.
[37] Wang C, Liu X, Demir NK, et al. Applications of water stable metal–organic frameworks. Chem Soc Rev 2016;45:5107–34.
[38] Férey G, Latroche M, Serre C, et al. Hydrogen adsorption in the nanoporous metal-benzenedicarboxylate $M(OH)(O_2C–C_6H_4-CO_2)$ (M = Al^{3+}, Cr^{3+}), MIL-53. Chem Commun 2003:2976–7.
[39] Jin L-N, Liu Q, Sun W-Y. Size-controlled indium (III)-benzenedicarboxylate hexagonal rods and their transformation to In_2O_3 hollow structures. CrystEngComm 2013;15:4779–84.
[40] Senkovska I, Hoffmann F, Fröba M, et al. New highly porous aluminium based metal-organic frameworks: Al(OH)(ndc)(ndc= 2,6-naphthalene dicarboxylate) and al (OH)(bpdc)(bpdc= 4,4′-biphenyl dicarboxylate). Micropor Mesopor Mater 2009;122:93–8.
[41] Thirumurugan A, Rao C. 1,2-, 1,3-and 1,4-Benzenedicarboxylates of Cd and Zn of different dimensionalities: process of formation of the three-dimensional structure. J Mater Chem 2005;15:3852–8.

Shaheed Ullah is currently working as a Ph.D. student in Prof. Xun Wang's group at the Department of Chemistry, Tsinghua University. He got his M.Phil. degree from Quaid-i-Azam University Islamabad Pakistan, in 2014 and M.Sc. Chemistry from the same institute in 2012. His current research interest is metal–organic framework nanostructures; their derived materials and applications.

Xun Wang received his Ph.D. degree from the Department of Chemistry, Tsinghua University in 2004. He then joined the faculty of the Department of Chemistry, Tsinghua University in 2004, and was promoted to an associate professor and full professor in 2005 and 2007, respectively. His current research interests include the synthetic methodology, formation mechanism, and properties of monodisperse nanocrystals.